

# **JMRA**





# Analytical Investigation Thermal and Mechanical Stresses of Steady-State in 2D-FGPPMS and 2D-PPMS for a Hollow Infinite Cylinder

# Mohsen Meshkini

Ph.D of Mechanical Engineering, Sharif University of Technology, International Campus (SUTIC), Kish Island, Iran Email: mohsenmeshkini.mmm@gmail.com

#### **Abstract**

This paper presents a lecture review on the analytical solution of steady-state thermomechanical behavior in a hollow infinite cylinder composed of functionally graded poropiezoelectric materials (2D-FGPPMs) and conventional poro-piezoelectric materials (2D-PPMs). The study is developed within the theoretical framework of two-dimensional thermoelasticity and aims to provide a comprehensive understanding of the coupled mechanical, thermal, and electrical responses of these advanced multi physics materials. To simulate realistic engineering conditions, general forms of thermal and mechanical boundary conditions are considered on both the inner and outer cylindrical surfaces. The analytical approach employs a direct solution method in which the governing heat conduction equation is solved simultaneously with the non-homogeneous system of partial differential Navier equations. Complex Fourier series expansion, in combination with power-law functions, is used to represent the distributions and to achieve accurate solutions for the asymmetric thermal and mechanical fields. In this formulation, all material properties—except for Poisson's ratio—are assumed to vary continuously along the radial and circumferential directions according to prescribed power-law distributions. This gradation reflects the functional nature of FGPPMs and captures the intricate coupling between poroelastic, piezoelectric, and thermal effects. The results of this investigation demonstrate the importance of FGPPMs in enhancing the design and optimization of highperformance engineering components. In particular, the findings highlight their potential applications

in the development of reliable sensors, actuators, and energy-harvesting devices that operate effectively under complex thermo-electro-mechanical environments [1,2].

**Keywords**: Functionally graded Material; Piezoelectric; Porothermoelastisity; Hollow cylinder.

#### 1.Introduction

Porous piezoelectric materials (PPMs) represent an important class of smart composites with the ability to couple mechanical, thermal, and electrical fields. Their reduced acoustic impedance makes them attractive for biomedical applications, such as ultrasonic imaging and sensors, while their multifunctionality ensures applicability in aerospace, oil and gas, and energy harvesting systems. Building upon these, functionally graded poro-piezoelectric materials (FGPPMs) have emerged as advanced structures where material properties vary continuously in two dimensions (radial and circumferential). This gradation enables superior stress distribution control, improved thermal resistance, and enhanced electromechanical coupling. The two selected studies form a coherent progression: from an analytical treatment of 2D-PPMs under thermo-electro-mechanical loading to the more advanced asymmetric mechanical and thermal stress analysis of 2D-FGPPMs hollow cylinders. Together, they present a significant foundation for understanding the mechanics of FGPPMs.

#### 2.Literature Background

Early works on FGMs and piezoelectric composites have shown their potential to mitigate thermal stresses and improve structural performance. Jabbari et al. developed general solutions for hollow cylinders under mechanical and thermal stresses, while other researchers investigated poro elasticity (Detournay & Cheng, Cowin) and piezo thermoelastic coupling (Ding, Kirilyuk). The studies under review here extend these frameworks by combining poroelasticity and piezoelectricity in both PPMs and FGPPMs.

#### 2.1 Asymmetric Mechanical and Thermal Stresses in 2D-FGPPMs Hollow Cylinder[1].

**Objective:** To extend the PPM framework to functionally graded materials with two-dimensional property variation.

**Method:** Analytical methods solving nonhomogeneous PDEs using complex Fourier series and power law functions. Material gradation is expressed via radial and circumferential power laws.

# **Key Features:**

- Inclusion of porosity, Biot's modulus, and electromechanical coupling.
- Material constants expressed as power functions of both radius and angle.
- General and particular solutions obtained for displacements, stresses, and electric potential.

#### Findings:

FGPPMs offer improved stress distribution and reduction of stress concentration compared to homogeneous or non-graded PPMs.

The effects of compressibility, porosity, and thermal expansion anisotropy are highlighted.

Results confirm that FGPPMs can be optimized for advanced thermal and mechanical performance.

# 2.2 Analytical Investigation of 2D-PPMs Hollow Cylinder under TEM Loading[2].

**Objective:** To derive analytical solutions for porous piezoelectric hollow cylinders subjected to thermo-electro-mechanical (TEM) asymmetric loading.

**Method:** The governing equations are based on two-dimensional thermo- elasticity. The solution employs Fourier series expansion and power-exponential functions to solve heat conduction and Navier equations.

#### **Key Features:**

- Material properties vary radially and circumferentially.
- Stress-strain relations incorporate Biot's modulus for poro elastic effects.
- Both compressibility and porosity are considered.

**Findings:** The study demonstrated that porosity and electric potential coefficients significantly influence displacement, stress distribution, and electric potential. The results established a baseline analytical framework for porous piezoelectric materials.

**Solution Methodology:** Complex Fourier series enable handling of asymmetric boundary conditions, while power-law or exponential grading functions represent material inhomogeneity. These analytical formulations produce closed-form expressions for displacement, stress, and electric potential distributions, serving as benchmarks for numerical methods.

# 3. Analytical Approaches and Governing Equations

Both studies rely on the two-dimensional Navier equations of thermo-elasticity, coupled with Maxwell's equations for electric fields. Key aspects include:

Strain-Displacement Relations: Defined in radial (r) and circumferential (θ) coordinates.

Stress-Strain Relations: Incorporating elastic constants, piezoelectric coupling coefficients, thermal moduli, and Biot's modulus for pore pressure effects.

Heat Conduction Equation: Solved under steady-state, asymmetric conditions with conductivity varying along r and  $\theta$ .

# 3.1 Basic Governing Equations for 2D-FGPPMs and 2D-PPMs [1,2]

$$\sigma_{rr} = \hat{C}_{11} \mathcal{E}_{rr} + \hat{C}_{12} \mathcal{E}_{\theta\theta} + e_{21} E_{r} - C_{1}^{T} T(r, \theta)$$

$$\sigma_{\theta\theta} = \hat{C}_{12} \mathcal{E}_{rr} + \hat{C}_{22} \mathcal{E}_{\theta\theta} + e_{22} E_{r} - C_{2}^{T} T(r, \theta)$$

$$\sigma_{r\theta} = 2\hat{C}_{44} \mathcal{E}_{r\theta} + e_{24} E_{\theta}$$

$$D_{rr} = e_{21} \mathcal{E}_{rr} + e_{22} \mathcal{E}_{\theta\theta} - \mathcal{E}_{22} E_{r} + g_{21} T(r, \theta)$$

$$D_{\theta\theta} = 2e_{24} \mathcal{E}_{r\theta} - \mathcal{E}_{21} E_{\theta} + g_{22} T(r, \theta)$$

$$\hat{C}_{ij} = C_{ij} + C_{M} \quad and \quad C_{M} = M \gamma^{2}$$

$$(3.1.1)$$

 $\it M$  is Biot's moduli. Also, to obtain the equilibrium equations in terms of the displacement components for the 2D-FGPPM and 2D-PPMs cylinder, the functional relationship of the material properties must be known. Because the cylinder material is assumed to be graded along the radial and circumferential direction, the coefficient of thermal expansion and electric constants are

assumed to be described with the power-exponential laws as 
$$\alpha = \alpha_0 \tilde{r}^{m_1} e^{n_1 \theta}$$
  $C_{ij} = \overline{C}_{ij} \tilde{r}^{m_2} e^{n_2 \theta}$   $K = k_0 \tilde{r}^{m_3} e^{n_3 \theta}$   $e_{2i} = \overline{e}_{2i} \tilde{r}^{m_4} e^{n_4 \theta}$   $\varepsilon_{2i} = \overline{\varepsilon}_{2i} \tilde{r}^{m_5} e^{n_5 \theta}$   $g_{2i} = \overline{g}_{2i} \tilde{r}^{m_6} e^{n_6 \theta}$ 

Where  $\tilde{r} = r/a$ , and "a" is the inner radius. (3.1.2)

# 3.2 Final Governing Equations for 2D-FGPPMs and 2D-PPMs [1,2]

$$\begin{split} \sigma_{\pi} &= \frac{1}{a^{m_{2}}} \sum_{\substack{q=-\infty\\q\neq 0}}^{\infty} \left[ \sum_{j=1}^{6} \left( \hat{C}_{11} \left( \eta_{qj} D_{qj} r^{\eta_{q}+m_{2}-1} + (\beta_{q_{1}} + m_{1} + 1) I_{q_{1}} r^{\beta_{q_{1}}+m_{1}+m_{2}} + (\beta_{q_{2}} + m_{1} + 1) I_{q_{2}} r^{\beta_{q_{2}}+m_{1}+m_{2}} \right) - \frac{\alpha_{0}}{a^{m_{1}}} \bar{C}_{11} (A_{qj} r^{\beta_{q_{1}}+m_{1}+m_{2}} + A_{q2} r^{\beta_{q_{2}}+m_{1}+m_{2}}) \\ &+ \hat{C}_{12} \left( (iq + n_{1})(X_{qj} + 1) D_{qj} r^{\eta_{q}+m_{2}-1} + \left( (iq + n_{1}) I_{q_{3}} + I_{q_{1}} \right) r^{\beta_{q_{1}}+m_{1}+m_{2}} + \left( (iq + n_{1}) I_{q_{4}} + I_{q_{2}} \right) r^{\beta_{q_{2}}+m_{1}+m_{2}} \right) - \frac{2\alpha_{0}}{a^{m_{1}}} \bar{C}_{12} (A_{q1} r^{\beta_{q_{1}}+m_{1}+m_{2}} + A_{q2} r^{\beta_{q_{2}}+m_{1}+m_{2}}) e^{n_{2}\theta} \\ &+ \bar{e}_{21} \left( (\eta_{qj}) Y_{qj} D_{qj} r^{\eta_{q}+m_{2}-1} + (\beta_{q_{1}} + m_{1} + 1) I_{q_{5}} r^{\beta_{q_{1}}+m_{1}+m_{2}} + (\beta_{q_{2}} + m_{1} + 1) I_{q_{5}} r^{\beta_{q_{2}}+m_{1}+m_{2}} \right) e^{n_{2}\theta} \\ &= e^{n_{1}\theta} \left[ e^{(iq+n_{1})\theta} \right] e^{(iq+n_{1})\theta} \end{split}$$

$$\begin{split} \sigma_{\theta\theta} &= \frac{1}{a^{m_2}} \sum_{\substack{q=-\infty \\ q \neq 0}}^{\infty} \left[ \sum_{j=1}^{6} \left( \hat{C}_{12} \left( \eta_{qj} D_{qj} r^{\eta_{qj} + m_2 - 1} + (\beta_{q_1} + m_1 + 1) I_{q_1} r^{\beta_{q_1} + m_1 + m_2} + (\beta_{q_2} + m_1 + 1) I_{q_2} r^{\beta_{q_2} + m_1 + m_2} \right) - \frac{\alpha_0}{a^{m_1}} \vec{C}_{12} (A_{q1} r^{\beta_{q_1} + m_1 + m_2} + A_{q2} r^{\beta_{q_2} + m_1 + m_2}) \right. \\ &\quad + \hat{C}_{22} \left( (iq + n_1)(X_{qj} + 1) D_{qj} r^{\eta_{qj} + m_2 - 1} + \left( (iq + n_1)I_{q_3} + I_{q_1} \right) r^{\beta_{q_1} + m_1 + m_2} + \left( (iq + n_1)I_{q_4} + I_{q_2} \right) r^{\beta_{q_2} + m_1 + m_2} \right) - \frac{2\alpha_0}{a^{m_1}} \vec{C}_{22} (A_{q1} r^{\beta_{q_1} + m_1 + m_2} + A_{q2} r^{\beta_{q_2} + m_1 + m_2}) \right) e^{n_2 \theta} \\ &\quad + \vec{e}_{22} \left( (\eta_{qj}) Y_{qj} D_{qj} r^{\eta_{qj} + m_2 - 1} + (\beta_{q_1} + m_1 + 1) I_{q_2} r^{\beta_{q_1} + m_1 + m_2} + (\beta_{q_2} + m_1 + 1) I_{q_4} r^{\beta_{q_2} + m_1 + m_2} \right) e^{n_2 \theta} \right] e^{(iq + n_1) \theta} \end{split}$$

$$\begin{split} & \sigma_{r\theta} = \frac{1}{a^{m_2}} \sum_{\substack{q = -\infty \\ q = 0}}^{\infty} \left[ \sum_{j=1}^{6} \bar{C}_{44} \Big( (iq + n_1) + ((\eta_{qj} - 1)X_{qj}) D_{qj} r^{\eta_{q} + m_2 - 1} + \Big( (iq + n_1)I_{q_1} + (\beta_{q_1} + m_1)I_{q_3} \Big) r^{\beta_{q_1} + m_1 + m_2} + \Big( (iq + n_1)I_{q_2} + (\beta_{q_2} + m_1)I_{q_4} \Big) r^{\beta_{q_2} + m_1 + m_2} \Big) e^{n_2\theta} \right. \\ & \left. - \bar{e}_{24} \Big( (iq + n_1)Y_{qj} D_{qj} r^{\eta_{q} + m_2 - 1} + (iq + n_1)I_{q_3} r^{\beta_{q_1} + m_1 + m_2} + (iq + n_1)I_{q_6} r^{\beta_{q_2} + m_1 + m_2} \Big) e^{n_2\theta} \right. \right] e^{(iq + n_1)\theta} \end{split}$$

$$\sigma_{zz} = \frac{1}{a^{m_{2}}} \sum_{\substack{q=-\infty\\q\neq 0}}^{\infty} \left[ \sum_{j=1}^{6} \left( \hat{\bar{C}}_{12} \left( \eta_{qj} D_{qj} r^{\eta_{qj}+m_{2}-1} + (\beta_{q_{1}} + m_{1} + 1) I_{q_{1}} r^{\beta_{q_{1}}+m_{1}+m_{2}} + (\beta_{q_{2}} + m_{1} + 1) I_{q_{2}} r^{\beta_{q_{2}}+m_{1}+m_{2}} + \left( (iq + n_{1}) I_{q_{3}} + I_{q_{1}} \right) r^{\beta_{q_{1}}+m_{1}+m_{2}} \right. \\ \left. + \left( (iq + n_{1}) I_{q_{4}} + I_{q_{2}} \right) r^{\beta_{q_{2}}+m_{1}+m_{2}} - \frac{3\alpha_{0}}{a^{m_{0}}} \bar{C}_{12} (A_{q_{1}} r^{\beta_{q_{1}}+m_{1}+m_{2}} + A_{q_{2}} r^{\beta_{q_{2}}+m_{1}+m_{2}}) \right) \right] e^{n_{2}\theta} \\ \left. + \bar{e}_{23} \left( (\eta_{qj}) Y_{qj} D_{qj} r^{\eta_{qj}+m_{2}-1} + (\beta_{q_{1}} + m_{1} + 1) I_{q_{5}} r^{\beta_{q_{1}}+m_{1}+m_{2}} + (\beta_{q_{2}} + m_{1} + 1) I_{q_{6}} r^{\beta_{q_{2}}+m_{1}+m_{2}} \right) e^{n_{2}\theta} \right] e^{(iq+n_{1})\theta}$$

$$\begin{split} D_{rr} &= \frac{1}{a^{m_{2}}} \sum_{\substack{q=-\infty\\q\neq 0}}^{\infty} \left[ \sum_{j=1}^{6} \left( \overline{e}_{21} \left( \eta_{qj} D_{qj} r^{\eta_{qj}+m_{2}-1} + (\beta_{q_{1}} + m_{1} + 1) I_{q_{1}} r^{\beta_{q_{1}}+m_{1}+m_{2}} + (\beta_{q_{2}} + m_{1} + 1) I_{q_{2}} r^{\beta_{q_{2}}+m_{1}+m_{2}} \right) \right. \\ &+ \overline{e}_{22} \left( (iq + n_{1}) (X_{qj} + 1) D_{qj} r^{\eta_{qj}+m_{2}-1} + \left( (iq + n_{1}) I_{q_{3}} + I_{q_{1}} \right) r^{\beta_{q_{1}}+m_{1}+m_{2}} + \left( (iq + n_{1}) I_{q_{4}} + I_{q_{2}} \right) r^{\beta_{q_{2}}+m_{1}+m_{2}} \right) \right) e^{n_{2}\theta} \\ &- \overline{\varepsilon}_{22} \left( (\eta_{qj}) Y_{qj} D_{qj} r^{\eta_{qj}+m_{2}-1} + (\beta_{q_{1}} + m_{1} + 1) I_{q_{5}} r^{\beta_{q_{1}}+m_{1}+m_{2}} + (\beta_{q_{2}} + m_{1} + 1) I_{q_{6}} r^{\beta_{q_{2}}+m_{1}+m_{2}} \right) e^{n_{2}\theta} \\ &+ \frac{\overline{g}_{21}}{a^{m_{1}}} (A_{q_{1}} r^{\beta_{q_{1}}+m_{1}+m_{2}} + A_{q_{2}} r^{\beta_{q_{2}}+m_{1}+m_{2}}) e^{(n_{1}+n_{2})\theta} \right] e^{(iq+n_{1})\theta} \end{split}$$

$$D_{\theta\theta} = \frac{1}{a^{n_2}} \sum_{\substack{q=-\infty\\q\neq 0}}^{\infty} \left[ \sum_{j=1}^{6} \overline{e}_{24} \Big( (iq+n_1) + ((\eta_{qj}-1)X_{qj} \Big) D_{qj} r^{\eta_{qj}+m_4-1} + \Big( (iq+n_1)I_{q_1} + (\beta_{q_1}+m_1)I_{q_3} \Big) r^{\beta_{q_1}+m_1+m_4} + \Big( (iq+n_1)I_{q_2} + (\beta_{q_2}+m_1)I_{q_4} \Big) r^{\beta_{q_2}+m_1+m_4} \Big) e^{n_4\theta} \right] \\ - \overline{\varepsilon}_{21} \Big( (iq+n_1)Y_{qj} D_{qj} r^{\eta_{qj}+m_5-1} + (iq+n_1)I_{q_5} r^{\beta_{q_1}+m_1+m_5} + (iq+n_1)I_{q_6} r^{\beta_{q_2}+m_1+m_5} \Big) e^{n_5\theta} + \frac{\overline{g}_{22}}{a^{m_1}} (A_{q_1} r^{\beta_{q_1}+m_1+m_6} + A_{q_2} r^{\beta_{q_2}+m_1+m_6}) e^{n_5\theta} \Big] e^{i(q+n_1)\theta} \Big]$$

# 4. Key Results and Comparisons

#### 4.1 FGPPMs and PPMs

**FGPPMs:** Enabled tailored stress distribution via property variation in two dimensions. This reduced stress concentrations and improved thermal resistance.

**PPMs:** Showed significant dependence of stress fields on porosity and Biot's modulus. However, lack of gradation limited stress mitigation.

#### 4.2 Thermal and Mechanical Coupling

Both studies confirmed strong thermo-electro-mechanical coupling. Elevated porosity increased displacements but decreased stiffness. Gradation in FGPPMs mitigated these effects.

#### 4.3 Practical Implications

FGPPMs allow customized designs for harsh environments such as oil wells, pipelines, and aerospace structures.

PPMs remain attractive for biomedical sensors due to their tunable acoustic impedance.

#### 5. Applications

- Oil and Gas Industry: FGPPMs can be used for pressure and temperature sensors in deep wells, combining mechanical robustness with sensitivity.
- Biomedical Engineering: PPM-based sensors in ultrasound imaging and diagnostics.
- Smart Structures: Adaptive aerospace components and energy harvesting systems.
- High-Temperature Environments: FGPPMs provide thermal shock resistance and durability.

# 6.Result and Discussion

#### 6.1 2D-FGPPMs[1]

Figure (1) shows the temperature distribution in the wall thickness along the radius and circumferential directions. The effect of the power-law index on the temperature distribution in the also shown in Figure (2). Also Figure (3,4) show the radial thermal stresses in the cross section of the cylinder. It is interesting to see that all components of stresses follow a harmonic pattern on the outside surface. The radial stresses is zero at the insider surface, due to the assumed boundary conditions. This figure is the plot of stresses versus  $\theta$  at  $r = \overline{r}$ . Figure (5) show the, hoop thermal stresses in the cross section of the cylinder. where the pore compressibility coefficient (B) is changed the other parameters are fixed. Figure (6) show these stresses based on the pore volume fraction ( $\phi$ ) is pore volume per total volume.

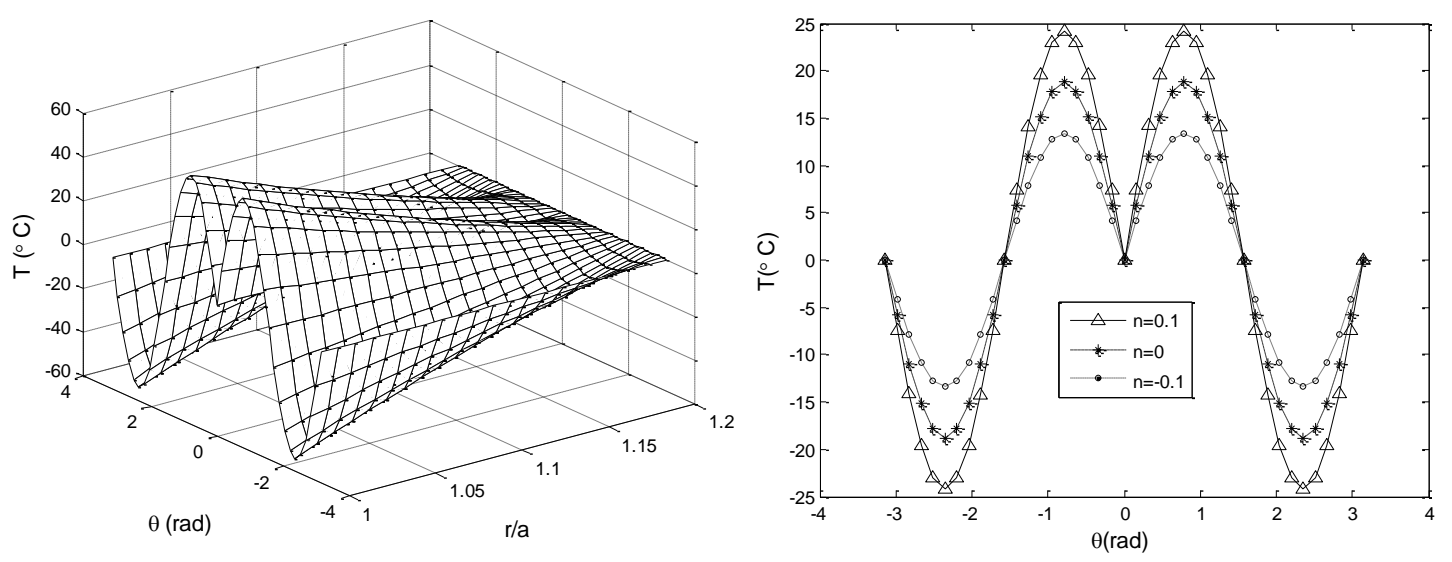


Fig.(1) Temperature distribution in the cross section of cylindrical Fig.(2) Temperature distribution of Circumferential at  $r = \overline{r}$ 

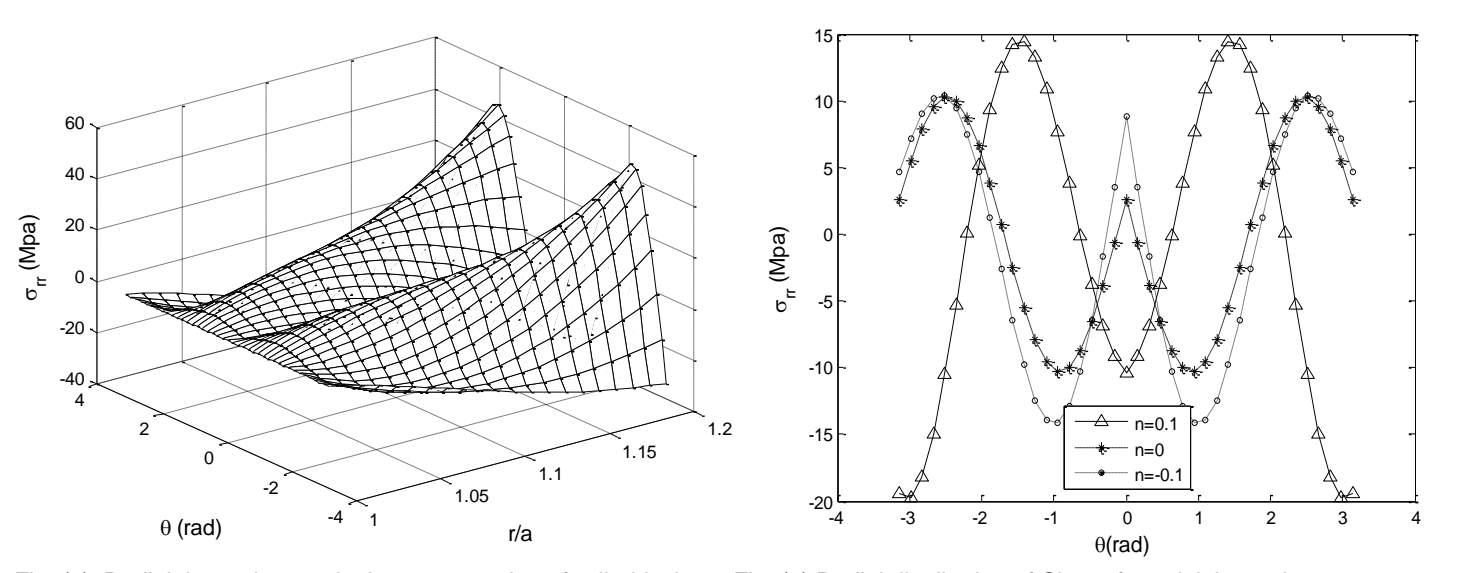


Fig .(3) Radial thermal stress in the cross section of cylindrical

Fig .(4) Radial distribution of Circumferential thermal stress  $\sigma_{rr}$  at  $r=\overline{r}$ 

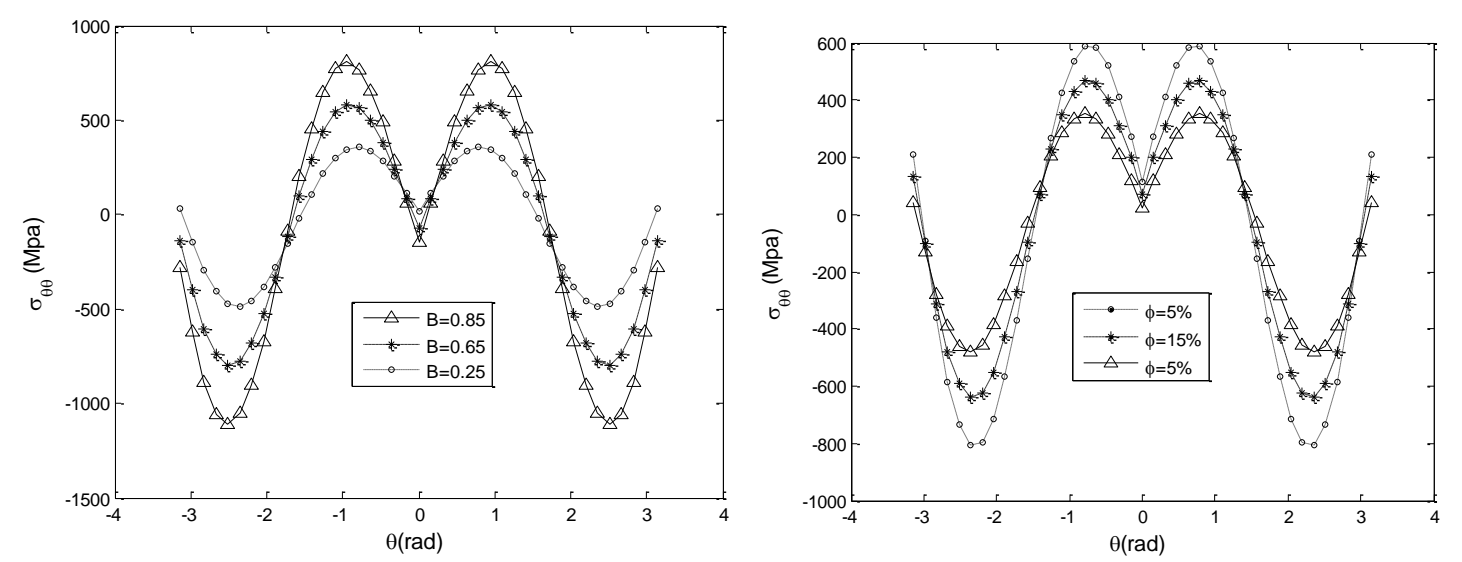
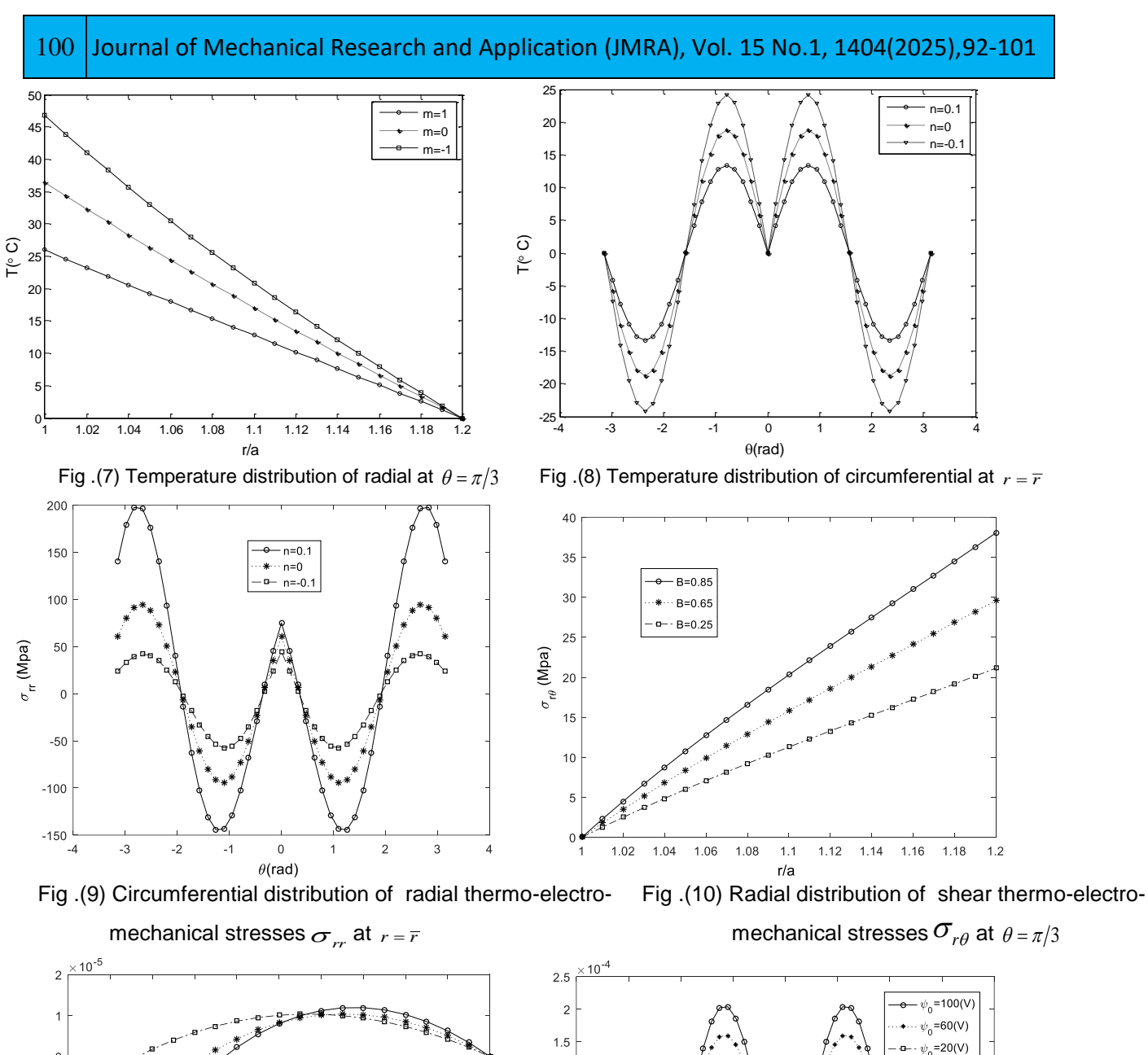


Fig .(5) Hoop thermal stress in the cross section of cylindr in diffrent compressibility coefficient.

Fig .(6) Hoop thermal stress in the cross section of cylinder in diffrent porosity cofficient.

# 6.2 PPM [2]

Figure (7),(8) shows the effect of the power- exponential law index on the temperature distribution in the wall thickness along the radius and circumferential directions. The effect of the power-exponential law index on the distribution of the radial thermo-electro-mechanical stresses is shown in Figure (9). It is shown that as m,n increases, the radial, hoop, shear and axial thermal stresses are increased. This figure is the plot of stresses versus  $\theta$  at  $r = \overline{r} = 1.1$  where  $\overline{r}$  is average inner radius "a" and outer radius "b". Figure (10) show the shear thermo-electro-mechanical stresses in the cross section of the cylinder, where the pore compressibility coefficient (B) is changed the other parameters are fixed. Figure (11) show the radial displacement in the cross section of the cylinder, where the based on the pore volume fraction ( $\phi$ ) changing. Figure (12) show the circumferential displacements in the cross section of cylinder, where the based on the versus electric potential coefficient ( $\Psi_0$ ) is changing.



2 ×10<sup>-5</sup>

2.5 ×10<sup>-4</sup>

2.5 ×10<sup>-4</sup>

2.5 ×10<sup>-4</sup>

2.5 ×10<sup>-4</sup>

2.5 ×10<sup>-4</sup>

2.6 ×10<sup>-4</sup>

2.7 ×10<sup>-4</sup>

2.8 ×10<sup>-4</sup>

2.9 ×10<sup>-4</sup>

3.0 ×10<sup>-4</sup>

3.0 ×10<sup>-4</sup>

3.0 ×10<sup>-4</sup>

4.0 ×10<sup>-4</sup>

5.0 ×10<sup>-4</sup>

6.1 ×10<sup>-4</sup>

7.1 ×10<sup>-4</sup>

8.0 ×10<sup>-4</sup>

9.1 ×1

Fig .(11) Radial distribution of  $\,\mathcal{U}\,$  with Different porosity coefficient at  $\,\theta=\pi/3\,$ 

Fig .(12) Circumferential distribution of V with electric potential coefficient at  $r = \overline{r}$ 

#### 7. Conclusion and Future Directions

The reviewed works highlight an attempt is made to study the problem of analytical solution for the 2D-FGPPM and 2D-PPMs hollow cylinder where the two-dimensional Asymmetric steadystate loads are implied. The analytical solutions provide deep insights into the coupled thermoelectro-mechanical behavior of hollow cylinders, serving as fundamental references for further research.[1,2]

#### 8. Future Research Directions:

- Extension to 3D geometries (spherical and conical shells).
- Dynamic and transient thermal-electrical analyses.
- Integration with numerical simulations (FEM, COMSOL) for complex boundary conditions.
- Experimental validation of theoretical models.
- Exploration of FGPPMs in multifunctional sensor and actuator design.

#### References

- [1] Meshkini, M., Firoozbakhsh, K., Jabbari, M. and SelkGhafari, A. (2016). "Asymmetric mechanical and thermal stresses in 2D-FGPPMs hollow cylinder". Journal of Thermal Stresses.
- [2] Meshkini, M., Firoozbakhsh, K., Jabbari, M. and SelkGhafari, A. (2018). "An Analytical investigation of 2D-PPMs Hollow Cylinder under Thermo-Electro-Mechanical Loadings", Journal of Theoretical and Applied Mechanics.

### **Biography:**

Mohsen Meshkini holds a PhD degree; he received his MS degrees in Mechanical Engineering from Islamic Azad University, South Tehran Branch, Tehran, Iran in 2011 and a PhD degree in the same field of study from Sharif University of Technology, International Campus (SUTIC), Kish, Iran in 2017.